Journal of Metals, Materials and Minerals, Vol. 30, No. 4, pp. 119-127, 2020

Influence of coconut shell powder organic reinforcement on chemical, microstructural and mechanical properties of spark plasma sintered Ti-Ni based metal matrix composite

Peter ODETOLA[1], Abimbola Patricia POPOOLA[1], Emmanuel AJENIFUJA[1,2,3,*], and Olawale POPOOLA[2]

[1] Department of Chemical, Metallurgical and Materials Engineering, Tshwane University of Technology, Pretoria West, Pretoria 0183, *South Africa.*

[2] *Center for Energy and Electric Power, Tshwane University of Technology, Pretoria, 0183, South Africa.*

[3] *Center for Energy Research and Development, Obafemi Awolowo University, Ile-Ife, 220005, Nigeria.*

***Corresponding author e-mail:** ajenifujae@tut.ac.za, eajenifuja@gmail.com

Received date:
9 June 2020
Revised date
15 September 2020
Accepted date:
16 September 2020

Keywords:
Titanium;
Nickel;
Spark plasma sintering;
Coconut shell powder;
Microhardness

Abstract

Metal matrix composites (MMCs) are currently used in place of pure alloys and polymer matrix composites because of their unique physical properties. Titanium and nickel powders were alloyed with coconut shell powder (CSP) as organic compound reinforcement to form a TiNi-based metal matrix composite (MMC) using spark plasma sintering (SPS) technique. The powders were mild-milled for 16 h and then axially consolidated at 850°C, heating rate of 100°C·min^{-1} and 50 MPa sintering pressure. Characterizations were done using field emission scanning electron microscope (FE-SEM-EDX) and x-ray diffractometer (XRD). Elemental and structural characterizations of the composites revealed the formation of the Ti-rich eutectic phase, Ni-rich dendrites, and TiNi-rich phase regions with dispersed distributions of carbides and oxide phases within the system. The Ni-rich "islands" appear to be depleted with increased CSP content. However, the relative density, tensile strength and microhardness improved in samples with higher amounts of CSP powder to the optimum values of 99.9%, 1022.91 MPa and 319.71 HV.

1. Introduction

Several hedges of breakthroughs are yet to be explored with the novel initiative of matrix reinforcement in composite technology for the development of excellent materials with a good combination of properties and superior performance in applications [1-5]. Over the years, success rates recorded in materials' usage especially in aerospace and automobile are still left with a huge vacuum to be filled with novel functional materials having cutting-edge innovations and sustainable performance to meet up with the current needs of the industries [6,7]. Generally, composites synergize the strengths of their components and eliminate their shortcomings to produce materials that fit the requirements for structures or applications that are especially exposed to extreme environments in terms of temperature, fluid, stress, and fatigue [8,9]. Titanium, nickel, and cobalt are metals with unique physical properties, and they are mostly reacted or combined with other materials to form ceramic, superalloy and intermetallics for different applications [10-14]. It is noted that MMCs are often more expensive than the conventional materials they are being replaced with, therefore, they are not widely applied, unless in a situation where performance can justify the added cost.

Coconut shell particles are very much available and have been used in different forms for several purposes. Naturally, they are hard and tough materials, with very high abrasion resistance, but despite its unique physical properties, limited findings have been recorded so far on the use of coconut shell particles or materials as reinforcement in metal matrix composites (MMCs) [15-17]. Meanwhile, coconut shell has been applied as reinforcements in other materials of mechanical and thermal importance [18-22]. Coconut shells are agricultural wastes that can constitute a nuisance to the environments, if not properly managed [1,4], most especially in tropical regions of the world. Therefore, the use of coconut shells as a replacement for conventional ceramic reinforcing materials would be a welcome development [4]. Coconut shells are cheap and readily available and can either be processed into powder [23,24] with an approximate density of 1.60 g·cm^{-3} or ash (CSA) with an approximate density of 2.05 g·cm^{-3}. Depending on the activation process, chemical analyses have shown that CSP materials are mainly composed of organic compounds and traces of ceramic materials after thermal conversion. Inorganic and ceramic components such as SiO_2, Al_2O_3, Fe_2O_3, CaO, MgO, and MnO have been found in substantial amounts, even above what is available in portland cement [18,19,25,26]. Therefore, naturally tough organic materials are attracting lots of interests as reinforcement in metal matrix composites like the advanced ceramic materials such as TiC, TiN, TiO_2, Si_3N_4, and SiC.

Metal matrix composites are often prepared by uniform dispersion of reinforcing materials within the metal matrix system using the common preparation techniques available such as casting, hot rolling, arc melting, etc. However, to obtain fully dense solid materials at relatively lower temperatures, spark plasma sintering, a non-conventional method, is an effective powder metallurgy method than other techniques [8,27]. SPS ensures good diffusional processes of powder

 DOI: 10.14456/jmmm.2020.60

mixtures to bridge the gap of adhesion problem between the organic-based coconut shell particles and the inorganic metal matrix phase due to poor wettability of the reinforcement phase [28,29]. To the best of the knowledge of the authors, no work has been reported on TiNi-CSP MMCs using the SPS powder metallurgy technique. In studies, expensive advanced ceramic compounds such as ZrO_2, TiN, SiB_6, TiB_2, B_4C, SiO_2, and CNT have been widely applied as metal matrix reinforcements, which makes the application of MMCs to be limited [7,28,30,31]. It is noteworthy that besides the cost of production, some advanced ceramics can be highly toxic in high concentrations. Hence, using organic materials as an alternative will markedly reduce the manufacturing cost, and will also increase the scope of application. This study aims to fabricate TiNi based metal matrix composite with the CSP as the reinforcement particulate source using spark plasma sintering technique and, hence investigate the effect of the reinforcement constituent variation on the chemical, morphology and mechanical properties of the sintered TiNi based metal matrix composites.

2. Materials and methods

2.1 Sintering procedure

Titanium and nickel powders (Alfa Aesar) with a purity of 99.99% and an average particle size of 10 μm were used as the matrix materials for the preparation of the metal matrix composite. A fixed weight percent of the titanium powder (50 wt%), however, the concentration of nickel was varied from 45 to 49 wt% of the amount of coconut shell powder (CSP) as organic reinforcement material. The samples were designated as CCS-T1, CCS-T2 and CCS-T3 for 1, 3 and 5 wt% amounts respectively. Tubular shaker mixer (T2F) operated at 72 rpm for 16 h was used to mild-mill the powders axially in a 250 ml cylindrical plastic container to ensure homogeneity. Based on calculations, appropriate amounts of powders required to form a metal matrix composite sample of 30 mm diameter and 5 mm thickness was charged into the graphite die and then sintered in a vacuum (5×10^{-2} mbar) environment using an automated spark plasma sintering (SPS) machine (HHPD – 25, FCT GmbH, Germany). The sintering parameters such as temperature, holding time, applied pressure and heating rate are given in Table 1. After sintering, the surface of the metal matrix pellets was cleaned off using sandblasting. The MMCs samples were sectioned into the required sizes, while other required metallurgical processes required for proper surface analysis were done. SEM-EDX analysis of the as-received elemental powders was carried out to ascertain the purity level of the matrix materials, and the microstructure images are shown in Figure 1.

2.2 Characterization Details

The cutting of the metal matrix composite samples to the required sizes was done using a precision CNC wire-cut electric discharge equipment. The samples were mounted in hardened polymer for easy handling for metallographic processes and analysis. The mounted specimens were ground in sequence with Rhaco Grit P320 and Aka-Rhaco using water as a medium at 300 rpm. The second stage of the grinding was done with Aka-Allegran 3 using DiaMaxx 6 μm Poly as the medium. Aka-Chemal in Fumed Silica was used for final polishing to the mirror-like surface and cleaned with distilled water. Hence the samples were etched with appropriate reagents for detail microstructural examination using a light microscope (Nikon ECLIPSE) and field-emission scanning electron microscope (JSM-7600F, JEOL) equipped with EDX for elemental and phase analyses. X-ray diffraction analysis of the samples was done using a Phillips diffractometer (PW 170) with Cu Kα radiation at 40 kV and 40 mA. The diffraction profile was analyzed with X'Pert High Score software. The mechanical properties of the samples were obtained using Future-Tech 700 Microhardness Tester (100 gf load at 10 s). The bulk density of the samples was determined using the Archimedes principle, while the densification was calculated relative to the theoretical density.

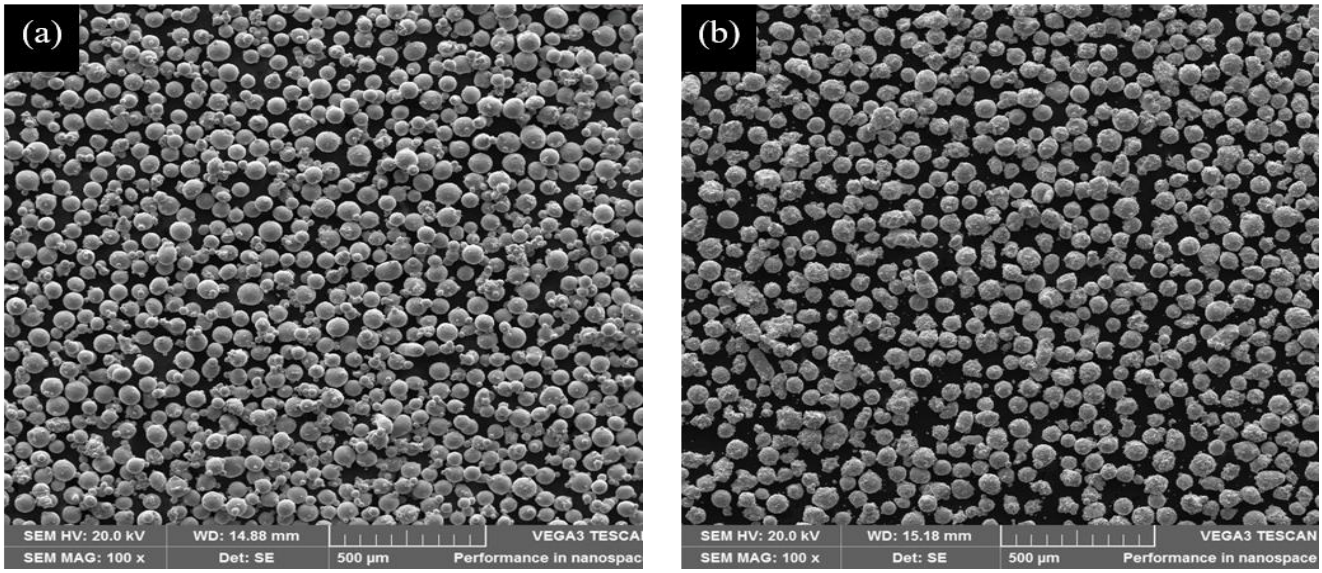

Figure 1. SEM micrographs of the metal matrix constituents for the MMCs (a) Ti and and (b) Ni.

Table 1. Sintering parameters and sintered relative densities of sintered TiNi/CCS composites.

SPS Parameters	Values
Sintering Temperature (°C)	850
Sintering Pressure (MPa)	50
Chamber Pressure (mbar)	5×10^{-2}
Heating rate (°C·min)	100
Holding Time (min)	10
Sintered Sample Density (%)	96.4, 98.9 and 99.9
Sample Thickness (mm)	5
Diameter (mm)	30

3. Results and discussions

3.1 Chemical Analysis

The physico-chemical analyses of coconut shells have been carried out by several authors [1-5,21,24]. Using several elemental characterization methods, its major compositions have been comparable, consisting mainly of the following oxides; Al_2O_3, MgO, SiO, CaO and Fe_2O_3. The qualitative and quantitative results as reported by different authors are similar. Meanwhile, the average elemental composition spectra obtained via EDX analysis of the sintered composite samples are shown in Figure 2-4 respectively for the samples. It is indicated qualitatively that the elemental composition of the sintered composites changed slightly corresponding to the initial constituents. The carbon content is shown to increase, while the presence of oxides is detected in samples CCS-T2 and CCS-T3, noting however that the oxygen content level in sample CCS-T1 may be below the detection limit of the EDX detector. The quantitative results corresponding to the EDX spectra are presented in Table 2. Also, on average, it is observed that the increase in the content of the reinforcing CSP material induced a proportional increase in oxides and carbides concentration in sintered samples. The oxides and carbides particles will provide grain boundary pinning effects in the metal matrix. Grain boundary pinning by reinforcement particles is often used to prevent grain growth during sintering or heat treatment procedures in metal matrix composites and alloys. Hence, the more the pinning particles in the matrix structure within the optimum range, the better the mechanical properties of the material. The arrangement or distribution of the phases within the material is identified on the micrographs as shown in Figure 2-4. Corresponding positions of the phases are indicated and are found to slightly change relative to the composite material composition. Chemical analysis of the phases revealed mainly the presence of carbon, oxygen, titanium, and nickel, whereas fluorine appears in sample CCS-T3 with 5 wt% of the organic reinforcement. Since the sintering experiment was carried out under a high vacuum environment, the non-metallic component and oxide phases are attributed to the organic reinforcement within the metal matrix. Meanwhile, traces of ceramic phases i.e. SiO_2, Al_2O_3, Fe_2O_3, $SiZrO_4$ are sparsely dispersed within the composite. The ceramic phases are believed to be formed by thermal decomposition and transformations of the coconut shell powder [18,19,26,32]. In all, three main phases were found as the primary dendrites, eutectic matrix and the boundary layer with their respective richness in Ti, Ni and TiNi intermetallics.

Table 2. Average EDX elemental composition of the metal matrix composites.

Elements	CCS-T1		CCS-T2		CCS-T3	
	Weight %	Atomic %	Weight %	Atomic %	Weight %	Atomic %
C k	6.97	24.77	7.15	21.42	9.24	19.07
O k	-	-	9.85	22.16	22.40	34.70
F k	-	-	-	-	16.22	21.15
Ti k	46.60	41.50	40.08	30.11	32.30	16.71
Ni k	46.42	33.73	42.92	26.81	19.83	8.37
Total	100					

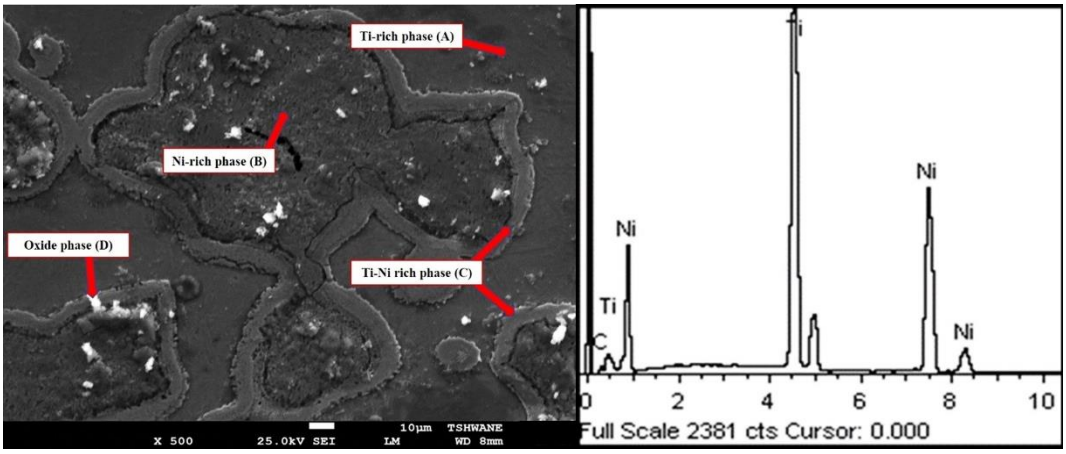

Figure 2. Phase identification and EDX elemental spectra for sample CCS-T1.

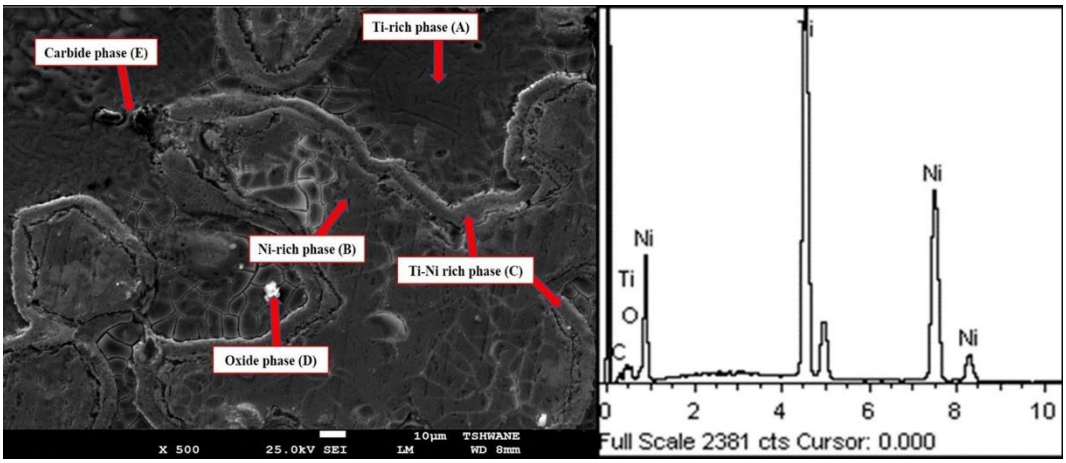

Figure 3. Phase identification and EDX elemental spectra for sample CCS-T2.

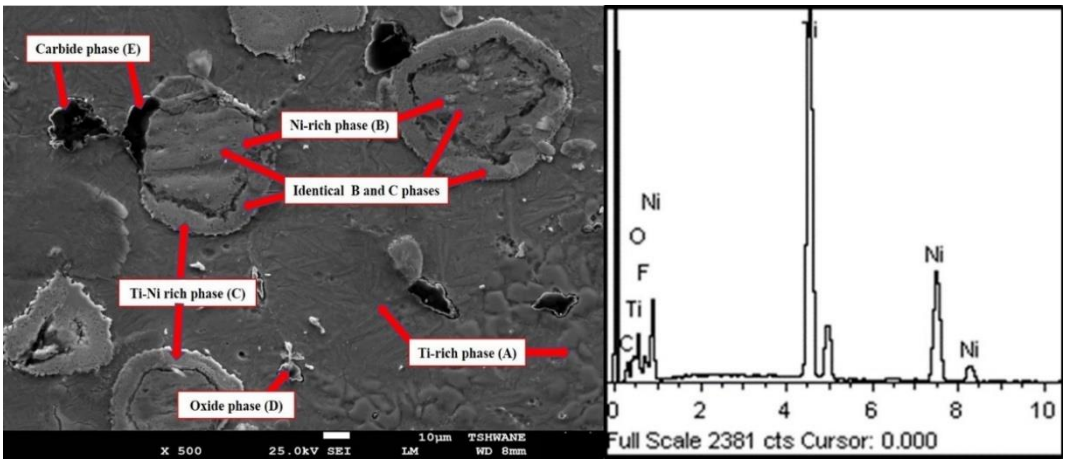

Figure 4. Phase identification and EDX elemental spectra for sample CCS-T3.

The randomly shaped dendritic phase is a nickel-rich "islands" designated as **B** on the micrograph (Figure 2-4). These partitioned Ni-rich dendrites are solid solution of Ti atoms in Ni and are well distributed within the continuous Ti-rich eutectic phase, noted as **A** on the micrograph. As the alloy cooled down, the Ni-rich nucleation sites grew as dendrites and solidified to become Ni-rich grains within the remaining eutectic microstructure with high Ti composition. Meanwhile, the other unique structure detected is the Ti-Ni rich intermetallic phase which is the boundary layer between Ti and Ni-rich compounds. The Ti-Ni rich phase was formed from the diffusion of Ti and Ni from either side of the partition as the alloy cooled. Also, there are dispersed ceramic particles i.e. oxide and carbide phases embedded in the composite. For instance, in sample CCS-T1, the elemental analysis of the "island" phase **B** gives the concentration of 60 wt% nickel, while the matrix phase **A** is highly rich in Ti with 92 wt% Ti and 8 wt% Ni. As shown in Figure 2, the distinct separation of the phases indicates phase partitioning induced by the spinodal decomposition. The boundary phase layer identified as **C** is intermediate in terms of composition between the two major phases **A** and **B**, which is the overlapping region between the phases in the metal matrix composite. Expectedly, the elemental analysis showed comparable concentrations of Ti and Ni at 49 wt% and 45 wt% respectively. The scantily distributed "white" crystallites in the samples, represented by **D** was identified to be composed of mainly nickel oxide. Meanwhile, the chemical analysis of the dark crystallites within the continuous matrix Ti-rich phase (**A**) observed in CCS-T3 shown Figure 4 was characterized to be a Ti-rich carbide compound, this is attributed to the solid-state reactions with CSP [10,33-35]. This is more prominent in sample CCS-T3, because of the higher concentration of coconut shell powder which added more carbon material as the main end-product. Also, the appearance of a distinct Ti-Ni rich boundary layer phase was noted to change more to the form of Ni-rich island phase, which gives an indication of the effect of reinforcement on the structure of the composite.

3.2 Microstructural Analysis

The photomicrographs of samples CCS-T1, CCS-T2 and CCS-T3 are presented in Figure 5. There is a change in the morphological characteristics of the composite samples with varied concentrations of coconut shell powder as shown in the images. The distribution of the "white" Ti-rich eutectic microstructure and dark grey (Ni-rich) primary dendrite phase can be seen, which indicates clearly microstructures facilitated by spinodal decomposition caused by

the thermal transformation at high temperature and pressure sintering. It is however noted that as the organic reinforcement increases, the nickel-rich dendrite phase becomes depleted, while the Ti-rich eutectic phase becomes more prominent. This is partly linked to the reduction in the concentration of nickel content as its being replaced with coconut shell powder, and possibly because of the higher reactivity of titanium compare to nickel in the system. The grain arrangement of Ti-rich and Ni-rich phases, and the changes that occurred at 3 and 5 wt% reinforcement contents in the metal matrix composites are observed in Figure 5(b-c). The separation boundary layer between the main phases in samples CCS-T1 and CCS-T2 are shown to be more visible than in sample CCS-T3, and the changes in the appearance could be attributed to the change in its chemical composition of the alloy. The mechanical and tribological properties can be linked directly to the material microstructures, i.e. grain refinement, size and phase distributions [36,37]. For instance, the decrease in the nickel content of the metal matrix shifted the solid solution transformation position, and thus it decreased the formation of the Ni-rich dendrite phase as the alloy cooled down. Also, the observed morphological evolution has shown that the addition of organic reinforcement influenced the physico-chemical properties of the TiNi metal matrix composite. The microstructure (Figure 5(c)) of CCS-T3 appears more uniform which indicated deleterious grain growth inhibition, i.e. the more the carbonized CSP microparticles, the more the pinning effects on the metal matrix particles during sintering. [38,39]. Also, an increase in the concentration of the reinforcement particles caused a change in the liquidus and eutectic transformation (reaction) temperature of the alloy as it diverges from a pure alloy (TiNi) system to a metal matrix composite which has a completely different thermodynamic property. The change in the fraction of the major phases (Ti-rich and Ni-rich) is presented in Table 3.

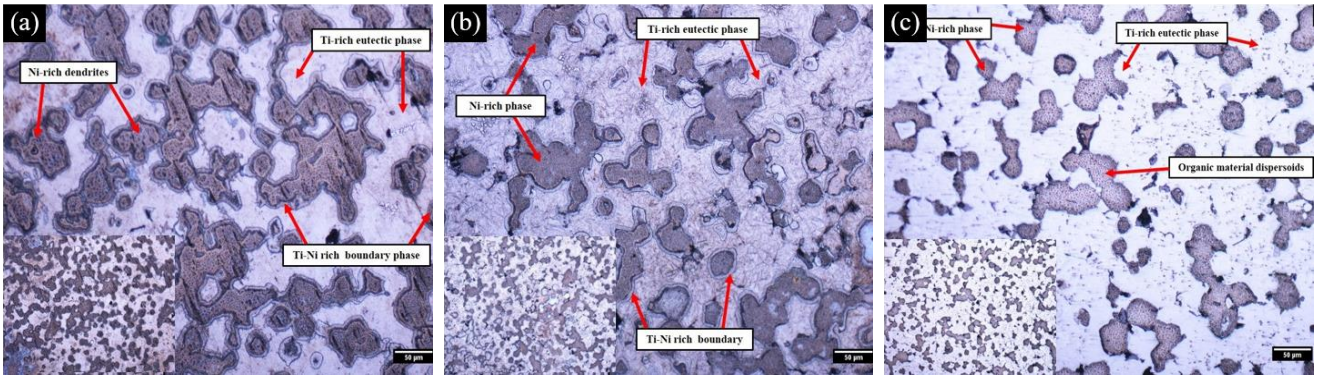

Figure 5. Photomicrographs for the TiNi based MMCs samples (a) CCS-T1, (b) CCS-T2 and (c) CCS-T3.

Table 3. Evolution in major phase fractions with the organic reinforcement contents.

Sample	Total Area (μm^2)	Average Size (μm)	% Area (Ni-rich)	% Area (Ti-rich)
CCS-T1	350438.99	141.42	49.53	50.47
CCS-T2	337787.33	87.99	41.08	58.92
CCS-T3	248066.55	104.45	32.31	67.69

The x-ray diffraction spectra of the samples are presented as shown in Figure 6. It is observed that all major phases detected are common to all samples. However, in agreement with microstructural analysis, peaks corresponding to $TiNi_3$ intermetallic were conspicuously absent in sample CCS-T3 (Figure 6(c)) with 5 wt% organic reinforcement. The diffraction patterns indicate that the samples are polycrystalline in nature with the existence of sharp crystallographic peaks corresponding to distinct phases at different 2θ°. The reflections are indexed and were shown to have preferred orientations at the planes observed at (020), (011), (111), (002) and (022) corresponding to the intermetallic compounds and oxides of titanium, nickel, and zircon. Meanwhile, other peaks are also observed at relatively low intensity indicating the presence of Ti_4Fe_2O and $TiNi_3$ intermetallic phases and silica compounds. This agrees with the chemical analysis which indicated the formation of three main phases with major constituents of Ti, Ni, and Ti-Ni. Besides, a higher concentration of the organic reinforcement impeded the formation of the $TiNi_3$ intermetallic alloy phase (the boundary layer between the Ti and Ni-rich phases). Though intermetallic compounds may possess good hardness properties, however, they are often avoided in some material requiring high toughness quality to avoid failure, because of their brittleness nature. Based on studies, the phase transformation induced by the carbonized natural material would enhance the mechanical property of the metal matrix composite [40]. Notably, substitution by amorphous carbon with a relatively smaller atomic radius (0.7 Å) from the CSP organic material would introduce lattice strain within the crystallographic structure of Ni and Ti with comparable atomic radii (1.67 and 1.47 Å respectively), and also induced amorphization of crystalline phase(s) i.e. the disappearance of peaks corresponding to $TiNi_3$ intermetallic phase with increase in the organic reinforcement (Figure 6(c)).

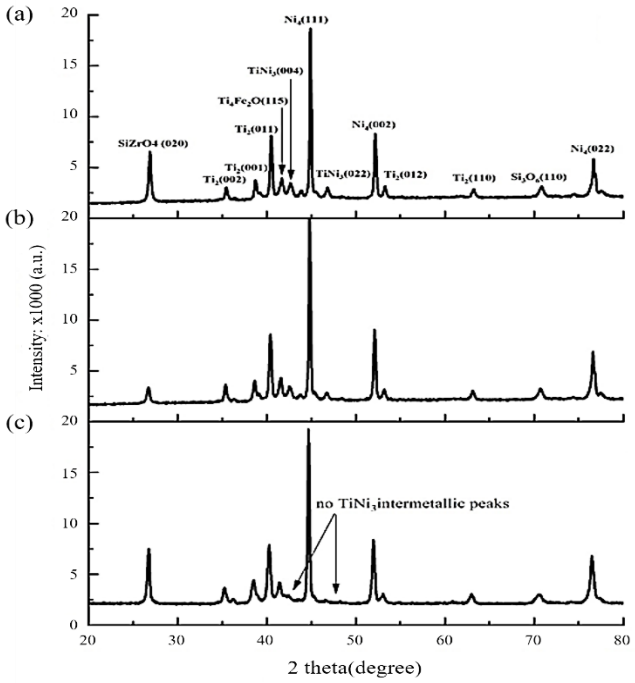

Figure 6. Representative XRD spectra for samples (a) CCS-T1, (b) CCS-T2 and (c) CCS-T3.

3.3 Mechanical Properties

The mechanical properties of the metal matrix composites were analyzed based on their relative density, microhardness, and tensile strength. The nominal microhardness values for Ti-Ni alloys are in the 200 HV range. However, with optimized transformation processes, mechanical properties can be greatly enhanced beyond the nominal values [41-42]. In this study, the relative density of the samples increased from 96.4% at (CCS-T1) to 98.9% (CCS-T2) with an optimum relative density of 99.99% for sample CCS-T3. It shows that, as the content of organic material in the Ti-Ni metal matrix increases, the microstructure of the composite became denser due to grain refinement. An increase in densification is attributed largely to the pinning influence of the carbonized coconut shell powder microparticles widely dispersed within the metal matrix. Unwanted grain growth within the metal particles is inhibited by the grain boundary pinning effect and thus induced a gradual physical transformation from a pure metal alloy to a metal matrix composite. Based on the foregoing, pores formation associated with the grain growth process was damped, thereby forming more a compact solid. The microhardness, relative density, and yield strength values are given in Table 4. For the microhardness analysis, ten indentations were done and the average value was taken for each sample. The lowest average HV value is 289.40, while the highest HV is 319.71 obtained at 5 wt% of CSP. These values are found to be higher than the nominal values for pure NiTi alloys [41-42]. The 3-D representations of the morphology of the samples are given in Figure 7, the change in the physico-chemical properties can be observed from the microstructural differences presented. It is noted that morphology becomes more compact and smoother with the increase in the CSP organic reinforcement.

To directly determine other mechanical properties of the samples, the relations between the hardness value, tensile and yield strengths given by Cahoon *et al.* was used [43,44] as in Equations (1) and (2). Hence, the tensile and yield strengths of the present Ti-Ni based metal matrix composite have been derived from their hardness values. The strain hardening coefficient, n, was taken to be 0.15.

$$TS = \left(\frac{H}{2.9}\right)\left(\frac{n}{0.217}\right)^{n} \quad (1)$$

$$YS = \left(\frac{H}{3}\right)(0.1)^{n} \quad (2)$$

The acronyms TS and YS are given as tensile and yield strengths respectively, and n is the strain-hardening coefficient. The TS and YS of the composite samples as calculated using the above expressions above are given in Table 4. Expectedly, the yield and tensile strengths increase accordingly with the addition of more reinforcement particles from the coconut shell material. Also, an illustration of the relationship between the amount of the organic reinforcement and the physico-chemical properties are shown in Figure 8.

The comparative analysis of the hardness properties and the yield strength values of some related Ti-based metal matrix composites (MMCs) are presented in Table 5. It is shown that the mechanical properties of the MMC samples prepared in this work are comparable to others given in earlier studies [12,45-49]. It is shown that composites with TiB and SiC reinforcements possess superior strength and hardness properties. However, the yield strength values in some cases decrease with the increase in the reinforcement quantity probably due to reduction in toughness [45-46,49]. Meanwhile, the MMCs with carbon fibre and carbon nanotubes (CNTs) [12,47] have relatively hardness and yield strength values compared to CCS-T samples..

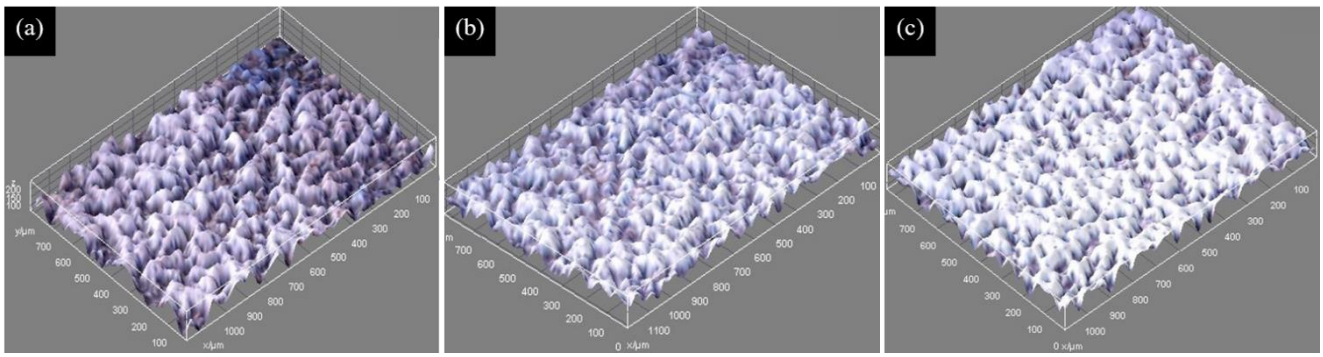

Figure 7. 3-D surface morphology of the MMCs (a) CCS-T1, (b) CCS-T2 and (c) CCS-T3.

Table 4. Relationship between sintered MMCs microhardness and CSP percentage weight.

Sample	CCS-T1	CCS-T2	CCS-T3
Carbonized Coconut shell (wt%)	1	3	5
Relative density (%)	96.4	98.9	99.9
Microhardness (HV)	289.40	296.81	319.71
Yield Strength (MPa)	669.75	686.90	739.90
Tensile Strength (MPa)	925.94	949.65	1022.91

Table 5. Mechanical Properties of Some Ti-based Metal Matrix Composites.

Metal Matrix	Reinforcement (wt%)	Microhardness (HV)	Yield Strength (MPa)	Reference
Ti-Ni (CCS-T1)	CSP (1)	289	670	
Ti-Ni (CCS-T2)	CSP (3)	297	687	
Ti-Ni (CCS-T3)	CSP (5)	320	740	
Ti	TiB (40)	768	140	[45]
Ti	TiB (60)	856	280	[45]
Ti	TiB (80)	1019	207	[45]
Ti	Carbon fibre (10)	214	274	[46]
Ti	CNTs (0.18)	275	682	[47]
Ti	CNTs (0.24)	278	704	[47]
Ti-Al-Mo-Fe	5% TiB	335	1038	[48]
Ti-Al-Mo-Fe	10% TiB	392	1147	[48]
Ti-Al-Mo-Fe	15% TiB	428	741	[48]
Ti	CNTs (1)	292	625	[12]
Ti	CNTs (2)	336	662	[12]
Ti	CNTs (3)	367	853	[12]
Ti-6Al-4V	SiC (5)	460	-	[49]
Ti-6Al-4V	SiC (10)	369	-	[49]
Ti-6Al-4V	SiC (15)	315	-	[49]

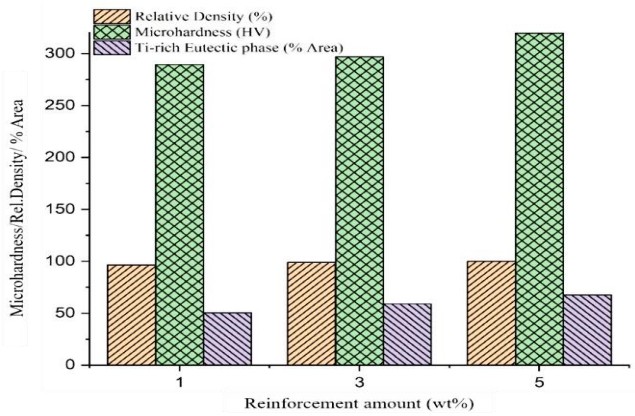

Figure 8. Relationship between the Ti-Ni composites densification and the microhardness.

4. Conclusions

Ti-Ni based metal matrix composite alloys have been prepared from high purity titanium and nickel elemental powders using coconut shell powder as the composite reinforcement. The fabrication was carried out under constant axial pressure using spark plasma sintering (SPS) at a relatively lower temperature (850°C). The effect of organic-based compositions on the metal matrix composite was investigated to study the chemical, microstructure and mechanical properties. Spinodal decomposition occurred within the composite material as noted with the phase partitioning of the microstructure into Ti-rich and Ni-rich compounds and separated by Ti-Ni intermetallic boundary. It is found that high concentrations impeded the formation of TiNi intermetallic. Also, the surface area covered by the Ti-rich compounds increases with the reinforcement addition. The micro-hardness properties and densification behaviour of the metal matrix composite samples improved with the CSP amount in the matrix. The improvement in mechanical behaviour is attributed to the effect of the synergy between the grain growth inhibition and grain boundary pinning by the dispersed reinforcement particles. The x-ray diffraction analysis indicates the absence of the TiNi intermetallic phase which agrees with the microstructural studies. Meanwhile, traces of oxides and ceramic compounds were detected as dispersoids within the metal matrix system.

Acknowledgments

The authors wish to thank Tshwane University of Technology (TUT), Pretoria, South Africa., for the supports provided during this work. Also, the support of the National Research Foundation (NRF), South Africa is hereby acknowledged.

References

[1] J.T. Utsev, and J.K. Taku, "Coconut shell ash as partial replacement of ordinary portland cement in concrete production," *International Journal of Scientific and Tecchnology Research*, vol. 1(8), pp. 86-89, 2012.

[2] L. Kumar, K.K. Pandey, and S. Khan, "Use of coconut shell ash as aggregates," *International Journal of Research in Engineering and Social Sciences,* vol. 7(2), pp. 15-19, 2017.

[3] U.J. Alengaram, B.A. Al Muhit, and M.Z. Jumaat, "Utilization of oil palm kernel shell as lightweight aggregate in concrete – A review," *Construction and Building Materials,* vol. 38, pp. 161-172, 2013.

[4] S. Ojha, G. Raghavendra, and S.K. Acharya, "Effect of Carbonized Coconut Shell Particles on Mechanical Properties of Bio-Based Composite," *Journal of Mineral Metal and Material Engineering,* vol. 2, pp. 6-10, 2016.

[5] K.S. Chun, S. Husseinsyah, and H. Osman, "Mechanical and thermal properties of coconut shell powder filled polylactic acid biocomposites: effects of the filler content and silane coupling agent," *Journal of Polymer Research,* vol. 19, pp. 9859, 2012.

[6] B.C. Bayer, D.A. Bosworth, B. Michaelis, R. Blume, G. Habler, R. Abart, R.S. Weatherup, P.R. Kidambi, J.J. Baumberg, A. Knop-Gericke, R. Schloegl, C. Baehtz, Z.H. Barber, J.C. Meyer, and S. Hofmann, "In situ observations of phase transitions in metastable nickel (carbide)/carbon nanocomposites," *Journal of Physical Chemistry C: Nanomater and Interfaces,* vol. 120(39), pp. 22571-22584, 2016.

[7] L. Qiao, W. Zhao, Y. Qin, and M. T. Swihart, "controlled growth of a hierarchical nickel carbide "dandelion" nanostructure," *Angewandte Chemie (International Edition in English),* 2016. DOI: 10.1002/anie.201603456.

[8] W.Y. Wu, C.W. Hsu, and J.M. Ting, "Nanoscaled C, Ni, Pt thin films," *Journal of Nano Research,* vol. 6(30), pp. 29-34, 2009.

[9] K. Sedláčková, P. Lobotka, I. Vávra, and G. Radnóczi, "Structural, electrical and magnetic properties of carbon-nickel composite thin films," *Carbon,* vol. 43(10), pp. 2192-2198, 2005.

[10] E. Ajenifuja, A.Y. Fasasi and G.A. Osinkolu, "Sputtering-pressure dependent optical and microstructural properties variations in dc reactive magnetron sputtered titanium nitride thin films," *Transactions of the Indian Ceramic Society,* vol. 71(4), pp. 181-188, 2012.

[11] E. Ajenifuja, G.A. Osinkolu, A.Y. Fasasi, D.A. Pelemo, and E.I. Obiajunwa, "Rutherford backscattering spectroscopy and structural analysis of DC reactive magnetron sputtered titanium nitride thin films on glass substrates," *Journal of Materials Science: Materials in Electronics,* vol. 27, pp. 335, 2016.

[12] K. Kondoh, T. Threrujirapapong, J. Umeda, and B. Fugetsu, "High-temperature properties of extruded titanium composites fabricated from carbon nanotubes coated titanium powderby spark plasma sintering and hot extrusion," *Composites Science and Technology,* pp. 129-1297, 2012.

[13] S. Li, B. Sun, H. Imai, T. Mimoto, and K. Kondoh, "Powder metallurgy titanium metal matrix composites reinforced with carbon nanotubes and graphite," *Composites Part A ,* vol. 48, pp. 57–66, 2013.

[14] Y. Yan, W. Jin, X.W. Li, J. Wang, and J.H. Liu, "Effects of pre-deformation and subsequent low-temperature annealing on transformation, mechanical properties and shape memory behavior of a Ti-rich TiNi alloy," *International Journal of Materials Research,* vol. 102, pp. 550-555, 2011.

[15] S. Chowdhury, A. Maniar, and O. M. Suganya, "Strength development in concrete with wood ash blended cement and use of soft computing models to predict strength parameters," *Journal of Advanced Research,* vol. 6, pp. 907-913, 2015.

[16] R. Siddique, "Utilization of wood ash in concrete manufacturing," *Resources, Conservation and Recycling* , vol. 67, pp. 27-33, 2012.

[17] E.O. Hall, "The deformation and ageing of mild steel: iii discussion of results," *Proceedings of the Physical Society London,* vol. 64(9), pp. 747-753, 1951.

[18] N.J. Petch, "The cleavage strength of polycrystals," *The Journal of the Iron and Steel Institute, London.,* vol. 173, pp. 25-28, 1953.

[19] M.S. Asl, Z. Ahmadi, S. Parvizi, Z. Balak, and I. Farahbakhsh, "Contribution of SiC particle size and spark plasma sintering conditions on grain growth and hardness of TiB_2 composites," *Ceramics International,* vol. 43, pp. 13924–13931, 2017.

[20] M.S. Asl, A.S. Namini, and M.G. Kakroudi, "Influence of silicon carbide addition on the microstructural development of hot pressed zirconium and titanium diborides,"*Ceramics International,* vol. 42, pp. 5375–5381, 2016.

[21] H. Salmah, M. Marliza, and P.L. Teh, "Treated coconut shell reinforced unsaturated polyester composites," *International Journal of Engineering & Technology,* vol. 13(2), pp. 94-102, 2013.

[22] E. Ajenifuja, A.P. I. Popoola, and O. M. Popoola, "Thickness dependent chemical and microstructural properties of DC reactive magnetron sputtered titanium nitride thin films on low carbon steel cross-section," *Journal of Materials Research and Technology,* vol. 8(1), pp. 377-384, 2019.

[23] M.E. Zeblon, E. Ajenifuja, and J.A. Ajao, "Thermal and microstructural study of slowly cooled Ni-B hard alloys containing," *Journal of Material Research and Technology,* vol. 8(1), pp. 359-365, 2019.

[24] T.L. Ting, R.P. Jaya, N.A. Hassan, H. Yaacob, D.S. Jayanti, and M. A. M. Ariffin, "A review of chemical and physical properties of coconut shell in asphalt mixture," *Jurnal Teknologi,* vol. 4, pp. 85-89, 2016.

[25] H.A. Abba, I.Z. Nur, and S. Salit, "Review of agro waste plastic composites production," *Journal of Minerals and Materials Characterization and Engineering,* vol. 1, pp. 271-279, 2013.

[26] S.A. Bello, I.A. Raheem, and N.K. Raji, "Study of tensile properties, fractography and morphology of aluminium (1xxx)/ coconut shell micro particle composites," *Journal of King Saud University – Engineering Sciences,* pp. 1018-3639, 2015.

[27] C. Cai, B. Song, P. Xue, Q. Wei, J.M. Wu, W. Li, and Y. Shi, "Effect of hot isostatic pressing procedure on performance of Ti6Al4V: surface qualities micro- structure and mechanical properties," *Journal of Alloys and Compounds,* vol. 686, pp. 55-63, 2016.

[28] R. Dungani, M. Karina, S.A. Subyakto, D. Hermawan, and A. Hadiyane, "agricultural waste fibers towards sustainability and advanced utilization: A review," *Asian Journal of Plant Sciences,* vol. 15(1-2), pp. 42-55, 2016.

[29] H. Feng, D. Jia, and Y. Zhou, "Spark plasma sintering reaction synthesized TiB reinforced titanium matrix composites," *Composites: Part A*, pp. 558-563, 2005.

[30] K.L. Firestein, S. Corthay, A E. Steinman, A.T. Matveev, A.M. Kovalskii, I.V. Sukhorukova, D. Golberg, and D.V. Shtansky, "High-strength aluminum-based composites reinforced with BN, AlB_2 and AlN particles fabricated via reactive spark plasma sintering of Al-BN powder mixtures," *Materials Science & Engineering A*, vol. 681, pp. 1-9, 2017.

[31] M. Geetha, A.K. Singh, R. Asokamani, and A.K. Gogia, "Ti based biomaterials, the ultimate choice for orthopedic implants-A review," *Progress in Materials Science*, vol. 54, pp. 397-425, 2009.

[32] S. Gorsse, and D.B. Miracle, "Mechanical properties of Ti–6Al–4V/TiB composites with randomly oriented and aligned TiB reinforcements," *Acta Materialia*, vol. 51, pp. 2427-2442, 2003.

[33] N.S. Karthiselva, S. Kashyap, D. Yadav, B.S. Murty, and S.R. Bakshi, "Densification mechanisms during reactive spark plasma sintering of Titanium diboride and Zirconium diboride," *Philosophical Magazine*, vol. 97(19), pp. 1588-1609, 2017.

[34] K. Kondoh, Titanium metal matrix composites by powder metallurgy (PM) routes, Osaka, Japan: Osaka University, *Joining and Welding Research Institute (JWRI)*, 2015.

[35] M.A. Lagos, I. Agote, G. Atxaga, O. Adarraga and L. Pambaguian, "Fabrication and characterisation of titanium matrix composites obtained using a combination of self propagating high temperature synthesis and spark plasma sintering.," *Materials Science & Engineering A*, vol. 655, pp. 44-49, 2016.

[36] M.A. Lagos, and I. Agote, "SPS synthesis and consolidation of TiAl alloys from elemental powders: microstructure evolution," *Intermetallics*, vol. 36, pp. 51-56, 2013.

[37] D.O. Moskovskikh, K.A. Paramonov, A.A. Nepapushev, N.F. Shkodich, and A.S. Mukasyan, "Bulk boron carbide nanostructured ceramics by reactive spark plasma sintering," *Ceramics International*, vol. 43(11), pp. 8190-8194, 2017.

[38] E.W. Neuman, G.E. Hilmas, and W.G. Fahrenholtz, "Processing, microstructure, and mechanical properties of zirconium diboride-boron carbide ceramics," *Ceramics International*, vol. 43(9), pp. 6942-6948, 2017.

[39] B.A. Obadele, O.O. Ige, and P.A. Olubambi, "Fabrication and characterization of titanium-nickel-zirconia matrix composites prepared by spark plasma sintering," *Journal of Alloys and Compounds*, vol. 710, pp. 825-830, 2017.

[40] S. Ranganath, "A review on particulate-reinforced titanium matrix composites," *Journal of Materials Science*, vol. 32, pp. 1-16, 1997.

[41] M. Zadra, and L. Girardini, "High-performance, low-cost titanium metal matrix composites," *Materials Science and Engineering: A*, vol. 608, pp. 155-163, 2014.

[42] C.J. Zhang, F.T. Kong, S.L. Xiao, E.T. Zhao, L.J. Xu, and Y. Y. Chen, "Evolution of microstructure and tensile properties of in situ titanium matrix composites with volume fraction of (TiB/TiC) reinforcements," *Materials Science and Engineering: A*, vol. 548, 2012.

[43] J.R. Cahoon, " An improved equation relating hardness to ultimate strength," *Metalurgical Transactions*, vol. 3, pp. 3040, 1972.

[44] J.R. Cahoon, W.H. Broughton, and K.A. R, "The determination of yield strength from hardness measurements," *Metallurgical Transactions A*, vol. 2(7), pp. 1979-1983, 1971.

[45] Z. Xinghong, X. Qiang, H. Jiecai, and V. Kvanin, "Self-propagating high temperature combustion synthesis of TiB/Ti composites," *Mater Sci Eng, A*, vol. 348(1-2), pp. 41–46, 2003.

[46] K. Geng, W. Lu, Y. Qin, and D. Zhang, "In situ preparation of titanium matrix composites reinforced with TiB whiskers and Y_2O_3 particles," *Mater Res Bull*, vol. 39(6), pp. 873-879, 2004.

[47] K. Kondoh, T. Threrujirapapong, H. Imai, J. Umeda, and B. Fugetsu, "Characteristics of powder metallurgy pure titanium matrix composite reinforced with multi-wall carbon nanotubes," *Compos Sci Technol*, vol. 69(7-8), pp. 1077–1081, 2009.

[48] Z. Yan, F. Chen, Y. Cai, and Y. Zheng, "Microstructure and mechanical properties of in-situ synthesized TiB whiskers reinforced titanium matrix composites by high-velocity compaction," *Powder Technol* , vol. 267, pp. 309-314, 2014.

[49] G. Sivakumar, V. Ananthi, and S. Ramanathan, "Production and mechanical properties of nano SiC particle reinforced Ti–6Al–4V matrix composite," *Trans Nonferrous Metals Soc China*, vol. 27(1), pp. 82–90, 2017.